Dynamical Influences on Cirrus Cloud Formation Process

HONG LIN

Atmospheric Environment Service, Downsview, Ontario, Canada

KEVIN J. NOONE AND JOHAN STRÖM

Department of Meteorology, Stockholm University, Stockholm, Sweden

ANDREW J. HEYMSFIELD

National Centre for Atmospheric Research, Boulder, Colorado

(Manuscript received 10 October 1996, in final form 30 July 1997)

ABSTRACT

An air parcel model has been used to study dynamic influences on cirrus cloud microphysical processes. Representative data selected from a measurement campaign carried out over southern Germany during March 1994 were used for a base-case model run where a modeled air parcel moved in a wave trajectory with a period similar to the measured Brunt–Väisälä frequency and an amplitude of about 30 m. Six case studies were performed for this paper. In each case, ice crystal nucleation processes were examined as an air parcel moved with trajectories having different wave forms. A random walk trajectory simulating turbulence with turbulent structure was also considered. The relationships between the parameters in the air parcel trajectories and crystal microphysical properties are discussed. Simulation results show that after two wave cycles, the model-produced crystal spectra are usually narrower than typical measurement data; however, broader spectra can be produced for certain types of trajectories. The broadness of crystal spectra is closely related to the air parcel's initial position in the wave trajectory. It is not necessary to invoke entrainment to produce a broad crystal spectrum.

1. Introduction

Cirrus clouds, located in the upper troposphere, play an important role in determining the earth's radiation budget and climate. The radiative properties of cirrus clouds depend strongly on their microphysical characteristics, particularly crystal size distribution, number concentration, and shapes of the crystals. Cirrus microphysical properties, especially the effective radius of the ice crystal, are important input parameters in climate models.

In situ measurements, especially those for small crystals, have been limited by the techniques and instruments used (Dowling and Radke 1990). The existence of high concentrations of small crystals ($\leq$30 μm) was seldom reported until recently by Noone et al. (1993), Ström and Heintzenberg (1994), Ström et al. (1994, 1997), and Heymsfield and Miloshevich (1995). In particular, the presence or absence of small crystals in cirrus clouds has been identified as an important aspect of the radiative properties of these clouds (Kinne et al. 1992; Zender and Kiehl 1994). The results from Zender and Kiehl (1994) showed that the shortwave forcing and albedo were very sensitive to the presence of small crystals (3–20 μm). This sensitivity could lead to uncertainties in the energy distribution in climate models. To treat cirrus clouds properly in climate models, it is necessary to understand the microphysical properties of cirrus crystals and their formation processes.

Modeling studies of cirrus formation processes have been carried out previously by Sassen et al. (1989), Heymsfield and Sabin (1989), Jensen et al. (1994), and DeMott et al. (1994). Homogeneous and heterogeneous nucleation processes of ice crystals have been discussed under different conditions and model results compared with field measurements. The consensus appears to be that heterogeneous nucleation could become important at warmer temperatures or in weak updrafts, but in lower temperature environments homogeneous nucleation dominates the crystal formation process.

Heymsfield and Sabin (1989) developed an air parcel model to study ice crystal homogeneous nucleation processes. This model has been used previously in an orographic wave study, where the temperature was low

Corresponding author address: D. Hong Lin, Atmospheric Environment Service, ARMP 4905 Dufferin Street Downsview, ON M3H 5T4, Canada.
E-mail: lin@armph3.tor.ec.gc.ca

($<-30°C$) and vertical updraft was strong (>2 m s^{-1}; Heymsfield and Miloshevich 1993), and later in a study of the influence of relative humidity and temperature on cirrus formation (Heymsfield and Miloshevich 1995). Their results were compared with in situ measurements and have shown the importance of homogeneous nucleation processes on crystal formation at lower temperatures. This model was later adapted to accept measured aerosol size distributions as inputs by Lin et al. (1998) to study the formation of small crystals in frontal cirrus that were observed in a campaign carried out over southern Germany during March 1994 (Ström et al. 1997). The model results showed the presence of numerous small ice crystals (diameter 1–20 μm) as had been observed in the experiment. The model results also showed that small aerosol particles (diameter < 0.1 μm) were active in forming cirrus cloud elements, also in agreement with the measurements.

In these previous studies, either a constant updraft velocity or wave trajectory with only a half wave cycle (i.e., the air parcel only went through one uplifting and descending process) was assumed. In reality, the wind flows in cirrus clouds are often turbulent (Gultepe and Starr 1995). Multiple wave structures were also observed (Ström et al. 1997). The dynamic forcing behind this type of velocity frequency or wave trajectory may have some impact on ice crystal microphysical properties. The effects of turbulence on cirrus nucleation processes are unknown. Unlike previous studies, multiple wave trajectories and random vertical velocities will be used in this paper to examine the influence of dynamic forcing on the crystal microphysical properties.

The focus of this paper is to examine the influence of dynamic forcing on the crystal microphysical properties. A cirrus parcel model (described previously by Lin et al. 1998) has been used in this study. Representative data selected from a measurement campaign carried out over southern Germany during March 1994 (Ström et al. 1997) are used for a base-case model run where the air parcel moved in a wave trajectory with a period similar to the measured Brunt–Väisälä frequency and an amplitude of about 30 m. We will present ice crystal size distributions, number concentrations, condensed water contents, and the properties of the scavenged and interstitial aerosols that resulted after using different air parcel trajectories in the model. The possibility of multiple crystal nucleation events in different air parcel trajectories, and the relationship between air parcel trajectories and the broadness of the model-produced crystal spectra will be investigated. A random walk trajectory (to simulate turbulence) will also be included in the discussion. The links between aerosol properties and cloud microphysics with respect to different dynamic forcing will be discussed.

TABLE 1. Model input values based on the observations taken on 18 March 1994 over southern Germany.

Pressure (hPa)	330
Altitude (m)	8500
Temperature (°C)	−51
Relative humidity (%)	85
Aerosol number concentration (cm^{-3})	350

2. Cirrus model and input parameters

The cirrus model used in this study was originally developed by Heymsfield and Sabin (1989). It was modified to accept aerosol size distributions as inputs by Lin et al. (1998) to simulate the formation of small crystals in cirrus clouds and to investigate aerosol–cloud interactions. The model consists of a system of ordinary differential equations [see Heymsfield and Sabin (1989) for detailed description] that describe both the microphysical properties of the droplets and ice crystals and the macrophysical properties of the air parcel. The model is set up as an initial value problem. Starting values include air parcel pressure, temperature, relative humidity, vertical velocity, and aerosol size distribution. Aerosol particles between 0.005 μm and 3 μm diameter are divided into 25 size bins. The model simulation begins when aerosol particles deliquesce in the air parcel. These aerosol particles are allowed to grow to equilibrium size before the air parcel moves. Droplets start to grow by water vapor diffusion as the parcel moves with a given vertical velocity. When the temperature becomes sufficiently low, ice crystals start to nucleate by homogeneous freezing of the solution droplets. The model assumes that all ice crystals are produced by homogeneous freezing, no preexisting ice crystals are introduced into the initial air parcel, and ice crystals do not sediment in the updraft.

In situ measurements made in frontal cirrostratus over southern Germany on 18 March 1994 (Ström et al. 1997) are used as a basis for model simulation. Similar to the Base-case initial condition in the previous study by Lin et al. (1998), we focus on the observation made on a flight during that day at 8500 m (pressure 330 hPa) level. At that level, an average temperature of $-51°C$ and an average relative humidity (respect to water) of 95% ($\pm 10\%$) were observed. The model initial environmental conditions are given in Table 1, where 85% relative humidity was used because the data analysis has shown that relative humidity was overestimated by about 10% in the observations. Two-minute average of the observed cloud residual and interstitial aerosol size distribution on 18 March was summed and used as the initial dry aerosol size distribution in the air parcel. The initial aerosol has a bimodal size distribution (thin solid line in Fig. 1d) and a number concentration of 350 cm^{-3}. In the model simulation, aerosol particles are assumed to be composed of ammonium sulfate and completely soluble.

Six case studies are included in this paper. All six

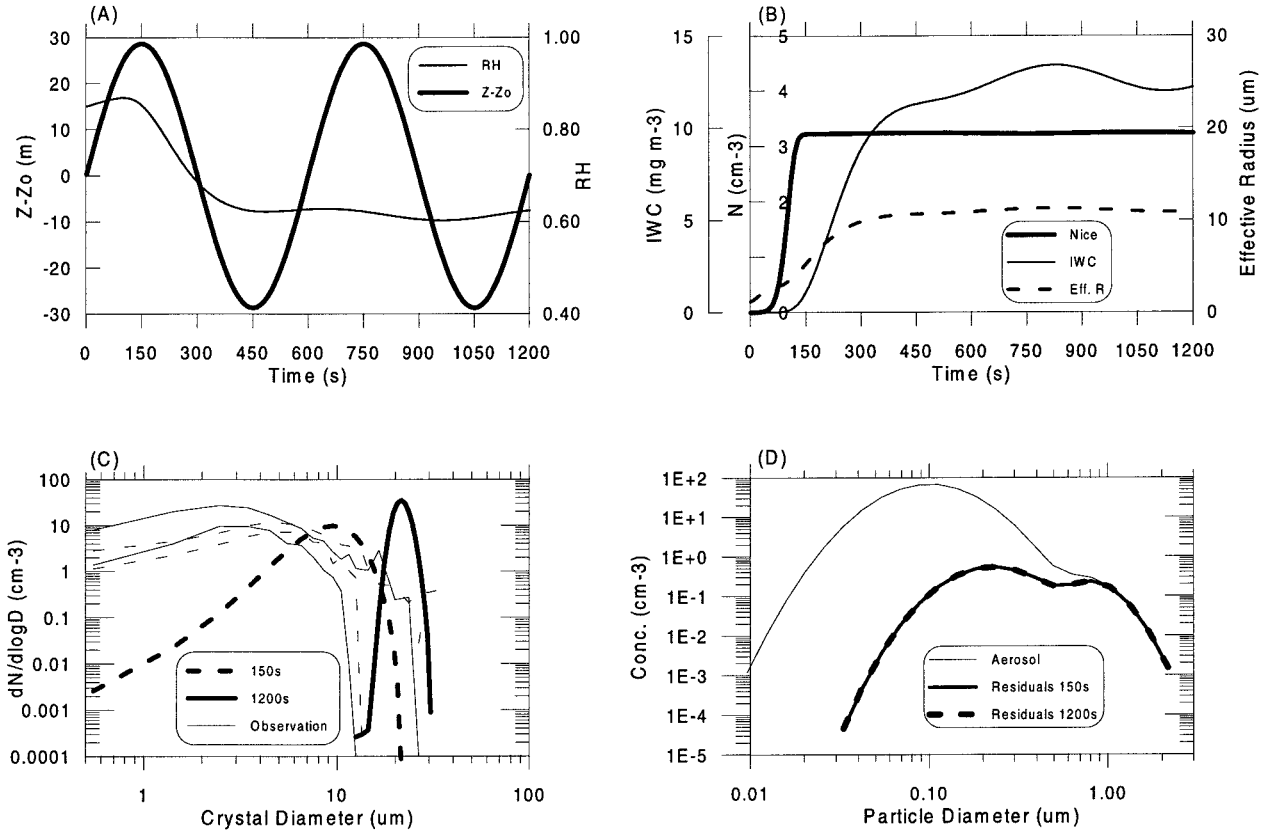

FIG. 1. Simulation results of case 1. (a) Air parcel wave trajectory and the temporal variation of relative humidity; (b) time histories of ice crystal number concentration, ice water content, and crystal effective radius; (c) model-produced ice crystal size distributions at 150 (thick dashed line) and 1200 s (thick solid line), along with two envelopes (areas between two thin solid lines and two thin dashed lines) of observed crystal size distribution from two regimes observed by using ice crystal replicator on 18 March 1994; and (d) residual aerosol size distributions at 150 and 1200 s (thick lines), and initial aerosol spectrum (thin solid line).

cases share the same initial input for the air parcel's environmental conditions and aerosol parameters and differ only in the air parcel trajectories. The air parcel trajectories were chosen based on the wave structure observed in cirrus clouds over southern Germany during the March 1994 campaign. On a particular day, 18 March, the bulk properties of the cloud appeared to be connected to wave structures in the vertical wind field consistent with the Brunt–Väisälä frequency. Analysis of potential temperature and vertical velocity suggested that the wave amplitude should be less than about 60 m and typically about 30 m. Case 1 is the base case simulation where a wave trajectory was chosen based on the wave structure observed in cirrus clouds on 18 March 1994. The air parcel trajectory has a period of 600 s and wave amplitude of about 30 m. Two wave cycles was used to study the impact of multiwave trajectory to the ice crystal formation and development. The wave trajectory in case 2 has an amplitude of about 60 m, twice the amplitude of the base case, which simulates a strong dynamic forcing on the air parcel. In case 3, a wave trajectory with two different wave amplitudes (about 10 m and 60 m) is used to examine the relationship between wave amplitude and nucleation processes. In case 4, a random walk trajectory derived from wind field data is used in order to explore the role of turbulence in the nucleation processes in an air parcel. The simulation results are compared with a smoothed random walk trajectory in case 5. Finally, a group of runs is conducted in case 6 for waves having the same amplitude and period as in the base case but initialized at different starting positions in the wave in order to study how that influences the broadness of crystal spectra. Using the results for these six cases, we wish to address the following questions.

1) Will crystals formed in the initial updraft keep growing, evaporate, or simply maintain their size in the rest of the wave cycles?
2) Do multiple nucleation events occur in multiwave trajectories?
3) Is it possible for this model to produce broad crystal spectra with a wave trajectory, or are processes that are not included in the model, for example, entrainment and aggregation, necessary to produce broader crystal spectra?

TABLE 2. Median values and ranges of crystal number concentration, ice water content (IWC), and aerosol scavenging fraction observed by the Counterflow Virtual Impactor (CVI) from four flights in March 1994 over Germany and two crystal effective radius calculated from replicator observations.

	Median values and (ranges)
Crystal (>5 μm) number concentration (cm^{-3}) STP*	2.5 (0.01–15)
IWC (mg cm^{-3}) STP	6 (0.1–100)
Aerosol scavenging fraction (crystals >5 μm) (%)	0.3% (0.01–10%)
Ice crystal effective radius (μm)	4 and 6**

* STP (standard temperature and pressure, 273.15 K and 1013.25 hPa) values are about a factor of 2.5 larger than their ambient values.

** These two effective radii were calculated by using the average of two groups of crystal size distributions observed from replicator measurements. Here, 4 μm is the effective radius of crystal distributions presented by thin dashed lines in Fig. 1c, 6 μm for thin solid lines.

3. Case studies

a. Case 1 (the base case): Air parcel trajectory having a wave structure with a constant amplitude

Case 1 (the base case) is defined based on observations in frontal cirrostratus over southern Germany by the German research aircraft Falcon on 18 March 1994 (Ström et al. 1997). On that particular day, the bulk properties of the cloud appeared to be connected to wave structures in the vertical wind field consistent with the measured Brunt–Väisälä frequency. Based on these observations, we assume that the air parcel has a vertical velocity (w: cm s^{-1}, t: s) given by $w = 30\cos(2\pi t/600)$. This vertical velocity gives the air parcel a corresponding wave trajectory (Fig. 1a) with a maximum amplitude of about 30 m and a period of 10 min.

Model simulation starts with an initial environment described in Table 1, and the air parcel follows the wave trajectory given in Fig. 1a. The temporal variation of relative humidity and the time histories of ice crystal number concentration, cloud ice water content (IWC), and ice crystal effective radius are shown in Figs. 1a and 1b. The peak value of relative humidity and maximum crystal number concentration is reached in the air parcel's first uplift (before 150 s). As the ice crystals nucleate and grow, they reduce the relative humidity, and nucleation is eventually shut off. There are no new ice crystals formed after the air parcel's first uplift (150 s) and crystal number concentration remains constant at 3.2 cm^{-3}.

Cloud IWC increases when crystals grow and decreases when crystals evaporate. As the crystals number concentration remains constant after the air parcel's first uplift, the decrease of IWC during air parcel's second descent (around 1050 s) indicates that some crystals have evaporated. However, there is no single ice crystal evaporated completely back to aerosol particles in this case.

TABLE 3. Model simulation results at two moments, 150 s and 1200 s, for all cases.

	Case 1		Case 2		Case 3		Case 4		Case 5		Case 6	
	Base-case wave trajectory		Wave amplitude doubled		Two different wave amplitudes		Random walk trajectory		Smoothed random walk trajectory		Base-case wave start at different position	
Time (s)	150	1200	150	1200	150	1200	150	1200	150	1200	150	1200
Crystal concentration (cm^{-3})	3.2	3.2	24.7	24.9	0.09	0.14	0.002	0.5	0.002	0.6	0.0005	2.7
IWC (mg m^{-3})	1.1	12.2	10.5	12.1	0.03	8.2	0.002	11.6	0.003	11.8	0.001	13.1
Aerosol scavenging (%)	0.9	0.9	7.1	7.1	0.03	0.4	0.0005	0.16	0.0004	0.18	0.0002	0.8
Effective radius (μm)	5.3	10.9	5.3	5.6	6.0	27.2	8.3	19.6	8.6	18.9	9.0	11.9

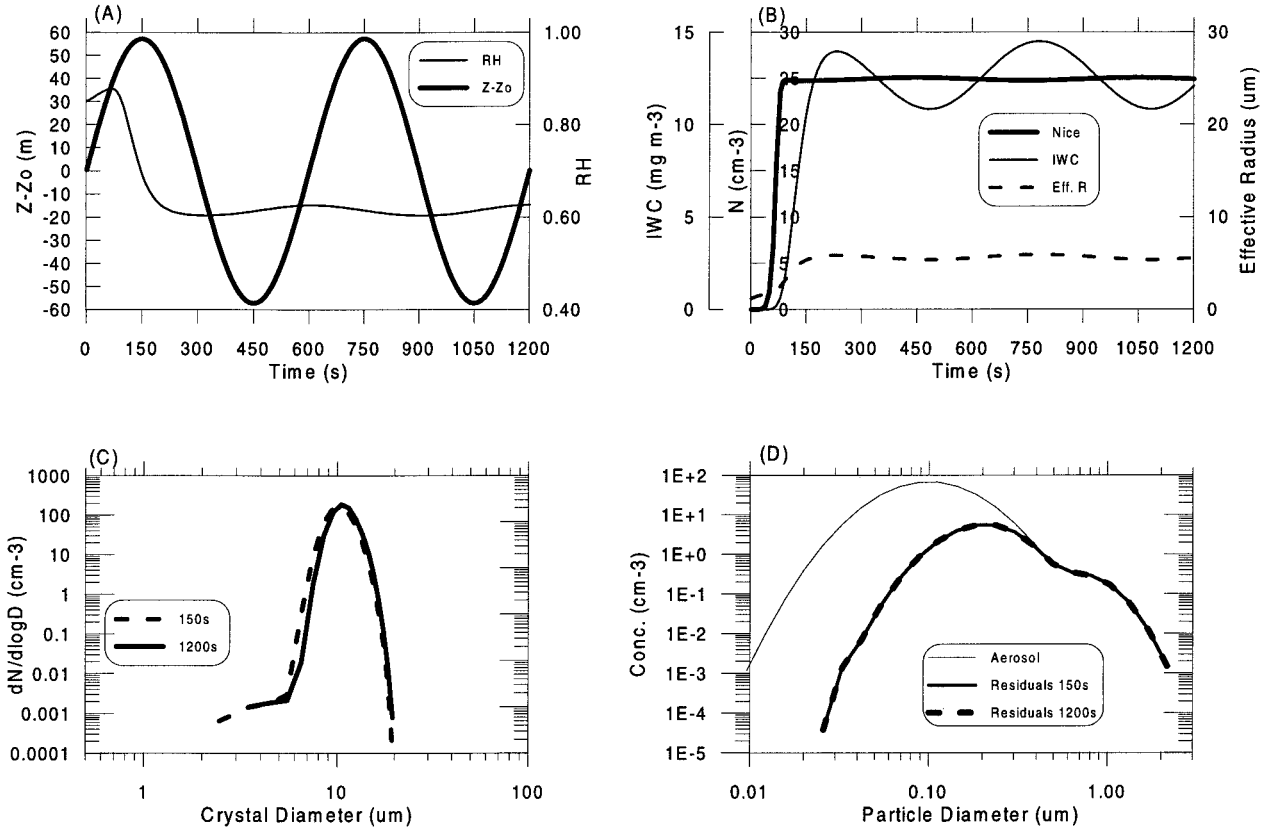

FIG. 2. Simulation results for case 2. (a) Air parcel trajectory with twice the amplitude as in the base case; (b) time histories of ice crystal number concentration, ice water content, and crystal effective radius; (c) model-produced ice crystal size distributions at 150 and 1200 s; and (d) the corresponding residual aerosol size distributions at 150 s and 1200 s (thick lines), and initial aerosol spectrum (thin solid line).

The ice crystal size distributions produced by the model after the first uplift (150 s) and after two wave cycles (1200 s) are shown in Fig. 1c by the heavy dashed and solid lines, respectively. Two areas between two dashed lines and two thin solid lines in Fig. 1c show the crystal size distributions from two regimes observed by replicator (Hallet 1976) on 18 March 1994. The crystal size spectrum at 150 s in Fig. 1b has a shape similar to the base case simulation in Lin et al (1998), where a constant vertical velocity is used and agrees with observation data for crystals larger than 5 μm. Since the replicator has sampling efficiency less than unity for crystals less than its cut size (about 4 μm), it is likely that the model underpredicted the number of crystals of this size. As the crystal nucleation is shut off after the air parcel's first uplift, small crystals could not be continuously produced. After two wave cycles (1200 s), the crystal spectrum becomes much narrower than both observations and the crystal spectrum at 150 s. However, after two wave cycles, the model-produced crystals are still in the size range of the observations.

Model-calculated residual size distribution at 150 and 1200 s, corresponding to the two crystal spectrums in Fig. 1c, are shown in Fig. 1d together with the initial aerosol size spectrum indicated by thin solid line. Residual size distributions at these two moments are overlapping. Again, it indicates that crystals neither nucleate nor evaporate back to aerosol particles after air parcel's first uplift.

For futher comparison, the crystal number concentration, IWC, and aerosol scavenging fraction observed in the same campaign in March 1994 (Ström et al. 1994) by using the Counterflow Virtual Impactor (CVI) are given in Table 2. In the table, median values and their typical ranges of measurement data obtained in a total of four flights are presented. Crystals number concentration and IWC are given by STP (standard temperature and pressure, 273.15 K and 1013.25 hPa) values that are about a factor of 2.5 larger than their ambient values. Crystals number concentration and aerosol scavenging fraction are only for crystals larger than 5 μm (CVI's cut size). Additionally, two ice crystal effective radii given in Table 2 were calculated from the average of two groups of crystal size distribution in Fig. 1c.

Model results at two moments, 150 s (after first uplift) and 1200 s (after two wave cycles), are summarized in Table 3 to compare directly with observations. Aerosol scavenging fraction, defined as the ratio of residual (aerosol particles on which the ice crystals are formed) number concentration to the initial aerosol number con-

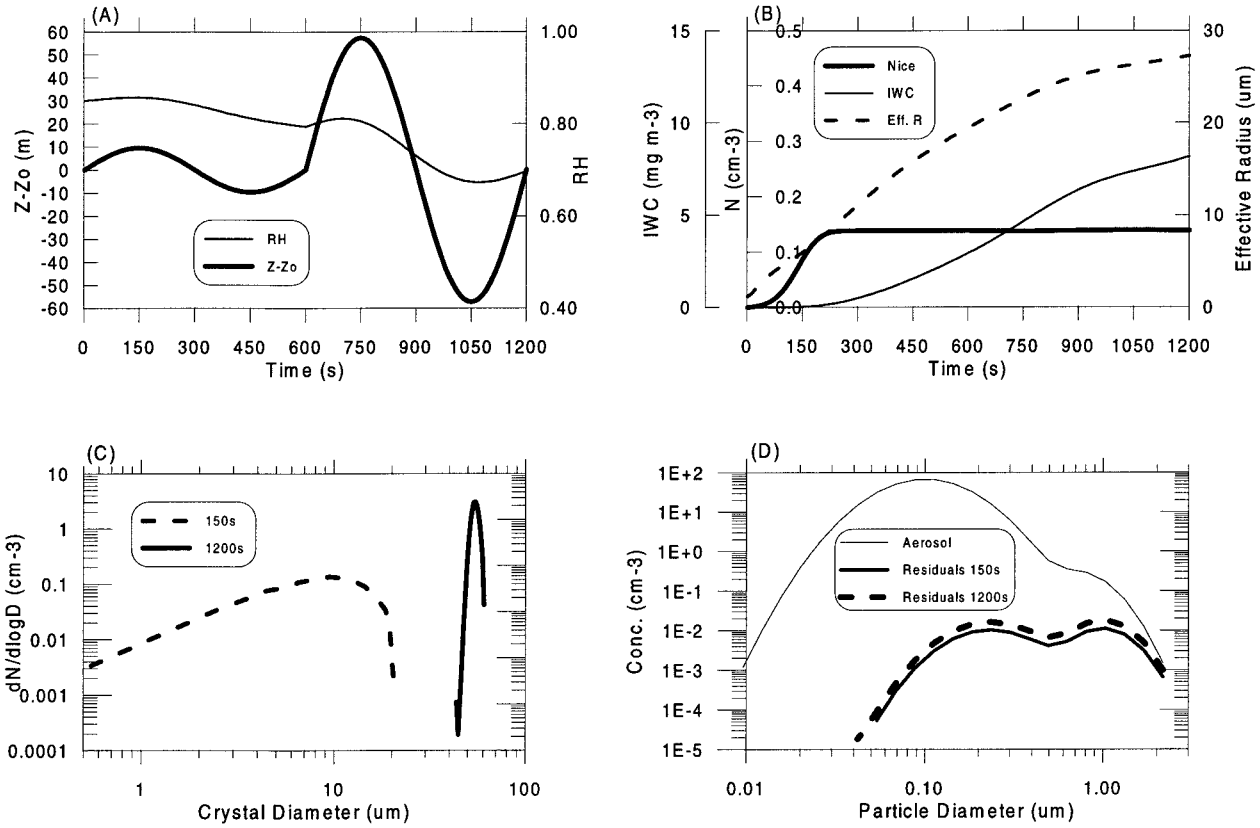

FIG. 3. Simulation results for case 3. (a) Air parcel trajectory with two different wave amplitude; (b) time histories of ice crystal number concentration, ice water content, and crystal effective radius; (c) model-produced ice crystal size distributions at 150 (dashed line) and 1200 s (solid line); and (d) the corresponding residual aerosol size distributions (thick lines) and initial aerosol spectrum (thin solid line).

centration, are also presented. In the case 1 simulation, 0.9% of the aerosol particles are scavenged by ice crystals, in agreement with observations. Model-produced crystal number concentrations at two moments are also in the range of observed crystal number concentration. However, IWC at 150 s is similar to observations, but the IWC after two wave cycles (1200 s) are much larger than the observation, as are the crystal effective radii.

In the case 1 simulation, we found that the wave trajectory with about 30-m amplitude did not produce any multiple nucleation events. The crystal spectrum is relatively narrow after two waves. However, crystal spectra often observed in cirrus clouds are broader than those produced by the model. To produce a broader crystal spectrum after two wave cycles, we may need multiple nucleation events to occur in the model simulation.

b. Case 2: Air parcel trajectory having wave structure with double the base-case amplitude

In case 2, a trajectory (shown in Fig. 2a) with twice the amplitude of the base case was chosen. Hence, the air parcel has a stronger vertical velocity $w = 60 \cos(2\pi t/600)$, which is also twice as much as case 1. The model simulation results are given in Figs. 2a–d and their values at 150 and 1200 s are summarized in Table 3 under case 2. There are 24.7 cm^{-3} crystals formed after the air parcel's first uplift (150 s), which is much greater than both the crystals nucleated in case 1, 3.2 cm^{-3}, and the observations. Obviously, strong updraft nucleates more crystals. But the crystal spectrum at 150 s is narrower than the crystal spectrum at 150 s in case 1. As larger-amplitude wave structure, or the stronger vertical velocity, have strong impact on the crystal nucleation, growth, and evaporation processes, the strong variations are also shown in the IWC (Fig. 2b).

The difference of crystal number concentration between 150 and 1200 s indicates that there are few ice crystals nucleated after the air parcel's first uplift. However, this additional nucleation is too weak and hardly affects the shape of the crystal spectrum. After two growth and evaporation cycles, the crystal size distribution at 1200 s is almost the same as the spectrum at 150 s.

The crystal effective radius in case 2 is quite stable (Fig. 2b). It only changes from 5.3 μm at 150 s to 5.6 μm at 1200 s and close to the observation values. However, the crystal spectrum is quite different from the

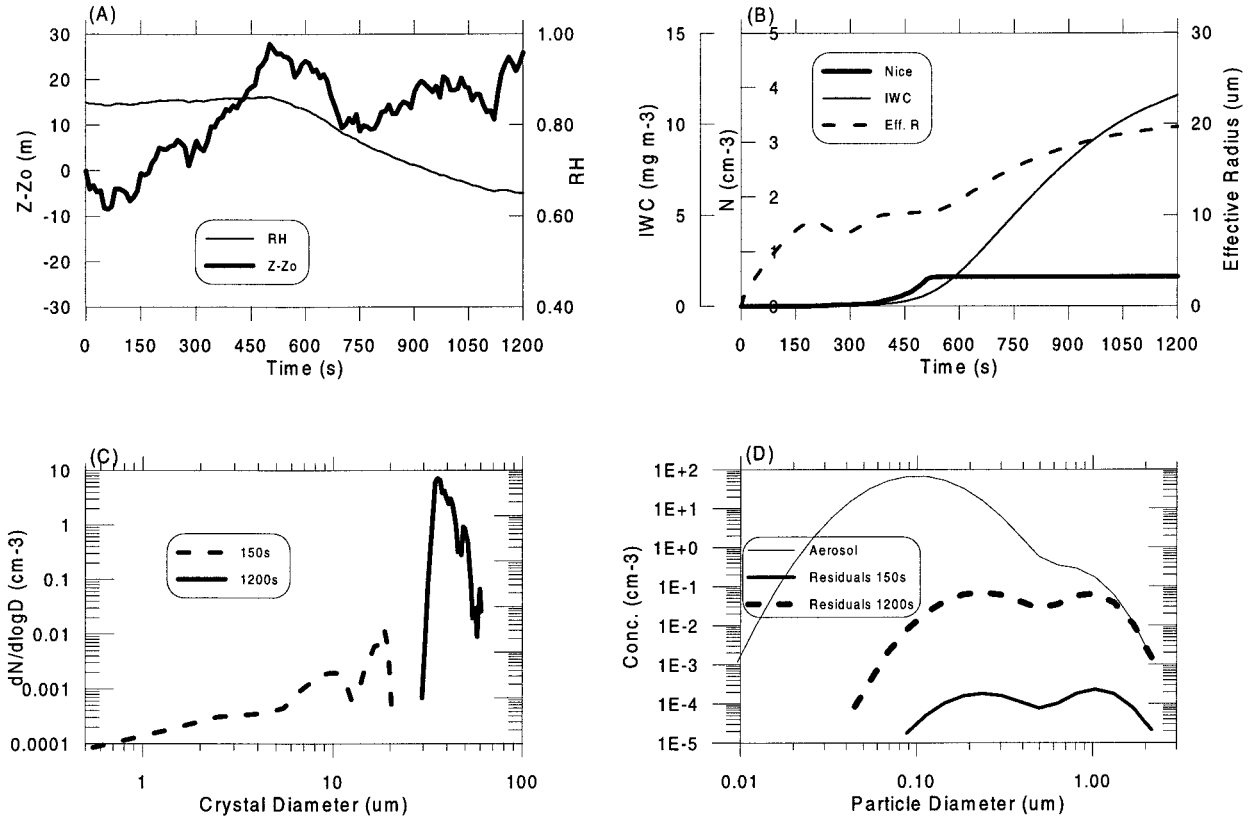

FIG. 4. Simulation results for case 4. (a) Air parcel random walk trajectory, (b) time histories of ice crystal number concentration, ice water content, and crystal effective radius; (c) model-produced ice crystal size distributions at 150 (dashed line) and 1200 s (solid line); and (d) the corresponding residual aerosol size distributions (thick lines) and initial aerosol spectrum (thin solid line).

observations. Doubling the wave amplitude does nucleate more crystals; however, it could not create a broader crystal spectrum.

c. Case 3: Air parcel trajectory having a wave structure with two different wave amplitudes

Weak updrafts produce fewer crystals than strong updrafts. To enable an additional nucleation event to occur, it may be necessary for only a small number of crystals to be produced in the first nucleation event. These few crystals could grow to large sizes without taking away so much water vapor that the homogeneous nucleation processes would stop. In case 3, an air parcel trajectory having a wave structure with two different amplitudes is tested. The air parcel has vertical velocities (w: cm s^{-1}) $w_1 = 10 \cos(2\pi t/600)$ for its first wave and follows by $w_2 = 60 \cos(2\pi t/600)$ for the second wave and the trajectory is shown in Fig. 3a.

The crystals produced by the model after initial uplift (150 s, Fig. 3c) have a similar spectrum and crystal effective radius (Table 3, case 3) as in case 1 but with a much lower crystal number concentration. After two wave cycles (1200 s), the crystal number concentration is higher than at 150 s (Fig. 3c and Table 3). The time variation of relative humidity (Fig. 3a) has not shown a rapid decrease as in previous cases after its peak values. Some new crystals are formed after the initial uplift of the air parcel. However, after two wave cycles (1200 s), crystals have larger size but the crystal spectrum is still narrow, and the total crystal number concentration was much lower than case 1 and the measurements. We also tested a wave trajectory having the larger amplitude in the first wave and the smaller amplitude in the second wave. With this wave structure, no additional nucleation occurs in the simulation and the crystal spectrum is narrow after two wave cycles.

From model simulations in cases 1, 2, and 3, we find it unlikely that the amplitude in the wave trajectory is a key parameter in producing broad crystal spectra. We wish to know whether the narrowness of the spectra depends on the fact that we use an idealized sinusoidal wave trajectory for the air parcels. The vertical velocities observed in cirrus clouds (Gultepe and Starr 1995; Ström et al. 1997) are more stochastic in nature than our sinusoidal wave trajectories. In case 4, we shall introduce a random walk trajectory in the model simulation to investigate whether turbulence is important in producing broad spectra.

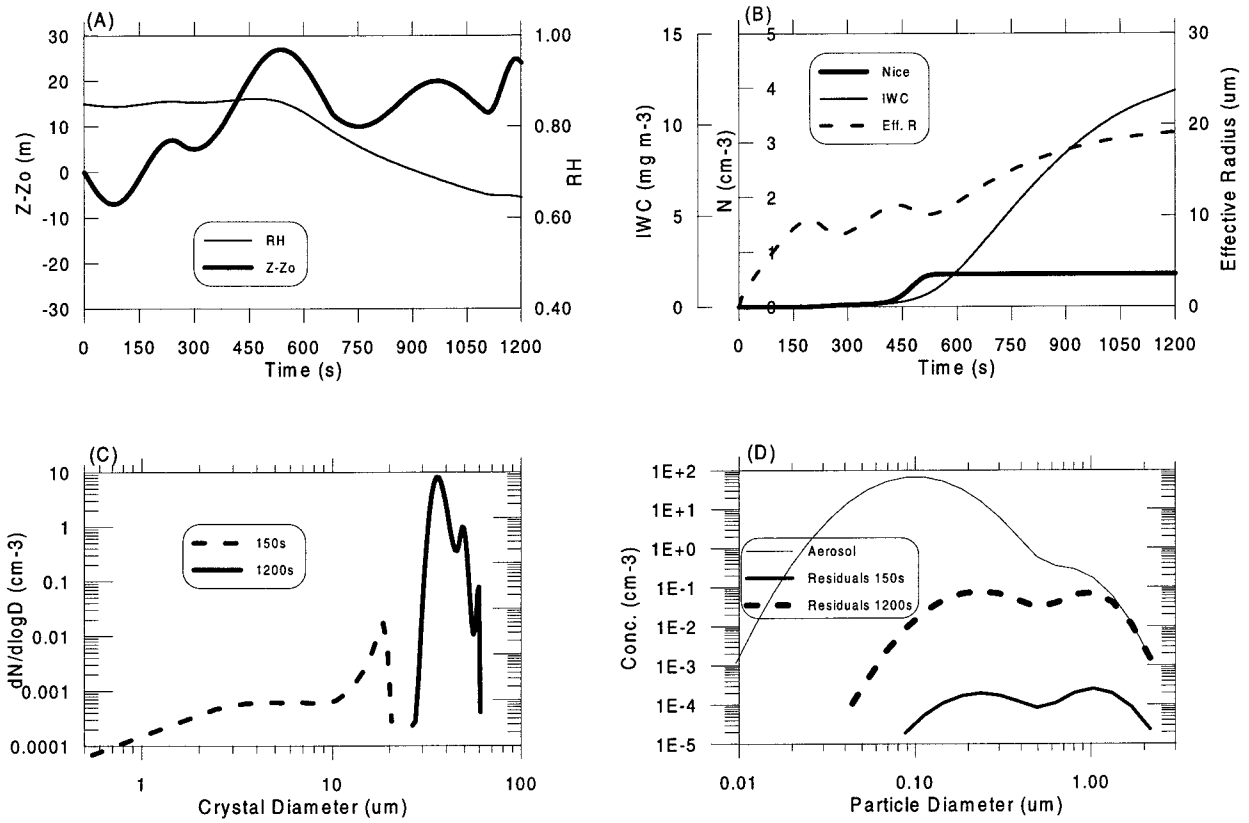

FIG. 5. Simulation results for case 5. (a) Air parcel with a smoothed random walk trajectory; (b) time histories of ice crystal number concentration, ice water content, and crystal effective radius; (c) model-produced ice crystal size distributions at 150 (dashed line) and 1200 s (solid line); and (d) the corresponding residual aerosol size distributions (thick lines) and initial aerosol spectrum (thin solid line).

d. Case 4: Air parcel having a random walk trajectory

In case 4, we generate a random vertical velocity for the air parcel. The random walk trajectory is shown in Fig. 4a. It has vertical amplitude of about 30 m. In this case, however, the air parcel descended slightly for about 10 m before the initial uplift. The model results are shown in Figs. 4a–d and Table 3 under case 4.

Initialized with a relative humidity of 85% at a temperature of $-51°C$, ammonium sulfate particles starts to deliquesce in the air parcel as in all other cases discussed previously. Deliquesced aerosol particles are allowed to grow to their equilibrium size before the air parcel starts moving. Generally, when an air parcel moves along a descending trajectory, the temperature will increase and relative humidity will decrease. This is the situation of the air parcel when it moves along the trajectory given in Fig. 4a. However, it is not necessary for all droplets to evaporate back to dry aerosol particles. As long as there are droplets in the air parcel, ice crystals will have chance to be nucleated by homogeneous freezing when temperature is still low enough. In case 4, the crystal spectrum has already shown two nucleation peaks at 150 s (Fig. 4c); however, the crystal number concentration is at this moment is extremely low (0.002 cm^{-3}, Table 3 under case 4).

As the trajectory descended in the very beginning, the occurrence of the peak value of relative humidity was delayed. In this case, the nucleation processes lasted longer before it shut down. The crystal size distribution at 1200 s is also shown in Fig. 4c. Crystals cover the size range 30–60 μm and there are several nucleation peaks in the spectrum. The crystal number concentration is also increased to 0.5 cm^{-3}, which is in the range of observation. However, the sizes of crystal are larger and the IWC is higher than both case 1 and the observation.

The crystal spectrum produced in this random walk trajectory is broader than the crystal spectra at 1200 s in all of the previous cases we discussed. The delayed ascent in the trajectory and the delayed occurrence of the peak relative humidity in the air parcel certainly allowed a few crystals to nucleate earlier. However, we still do not know how important the stochastic nature of the updraft velocity is to the broadness of the crystal spectrum.

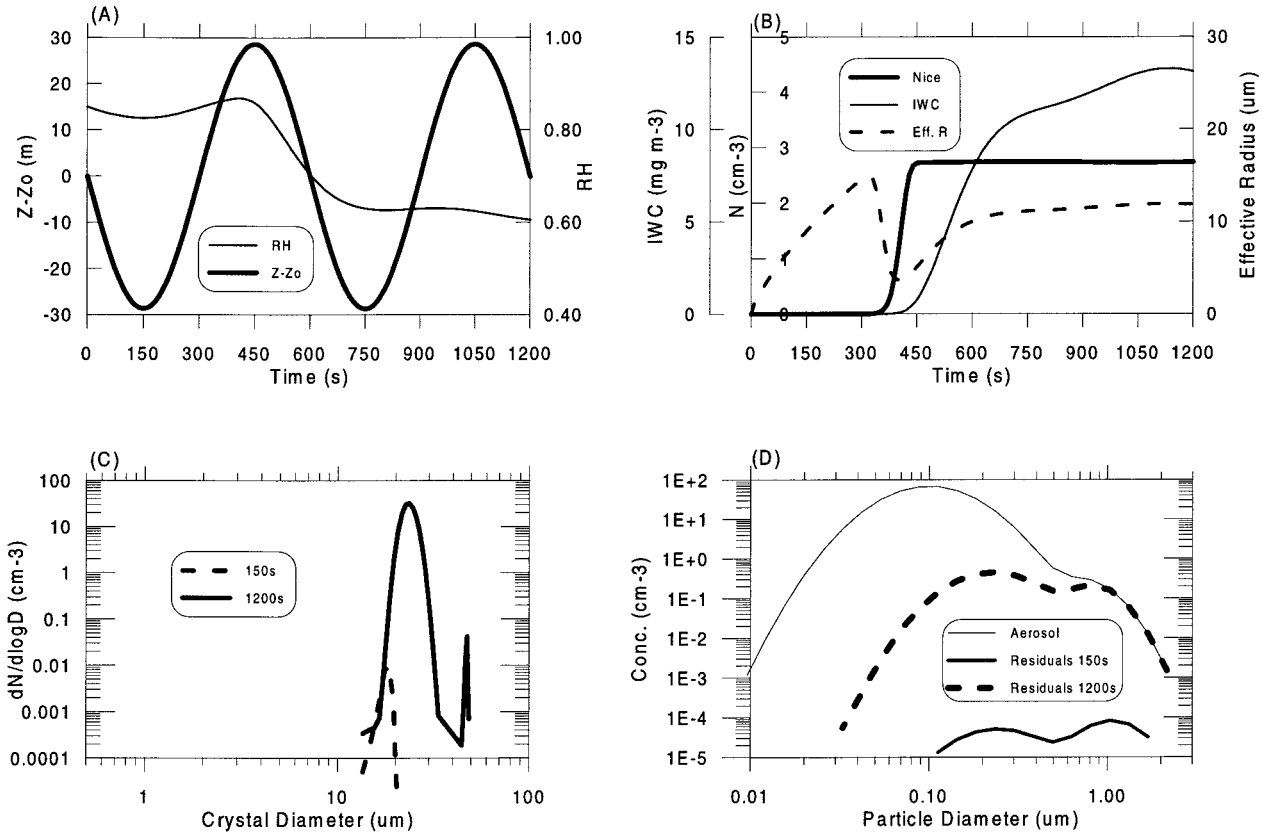

FIG. 6. Simulation results for case 6. (a) Air parcel starting with a position having wave phase $\varphi = \pi$, (b) time histories of ice crystal number concentration, ice water content, and crystal effective radius; (c) model-produced ice crystal size distributions at 150 (dashed line) and 1200 s (solid line); and (d) the corresponding residual aerosol size distributions (thick lines) and initial aerosol spectrum (thin solid line).

e. Case 5: Air parcel having a smoothed random walk trajectory as in case 4

To investigate the relationship between the small-scale (or stochastic) nature of a turbulent trajectory and the broadness of the crystal spectrum, the random walk trajectory in case 4 is smoothed by using a combination of four cosine wave functions. The smoothed random walk trajectory is shown in Fig. 5a and model simulation results are presented in Figs. 5a–d and Table 3 under case 5.

Results from the smoothed trajectory captured the main feature of the results from the random walk trajectory case, especially the three peaks in the crystal spectrum at 1200 s. However, it missed the small structure related to turbulence. For example, the crystal spectrum at 150 s in case 4 has two peaks, but one of them is smoothed out in case 5.

As the main results for cases 4 and 5 are so similar, we conclude that it is not the small-scale variations in the random walk trajectory that broaden the crystal spectrum but rather the path of the trajectory itself. It appears that a flat or an initially descending trajectory allows multiple or additional nucleation events to occur. This suggests that the initial position in a wave trajectory or the history of the air parcel could be a key parameter related to producing a broad spectrum.

f. Case 6: Air parcel trajectory having a wave structure as in the base case but different initial position in the wave trajectory

Case 6 includes three tests; each of them follows the same wave as the base case but starts at different initial positions. The vertical velocity (w: cm s^{-1}; t: s) is given by $w = 30\cos(2\pi t/600 + \varphi)$, where φ is the initial phase. The trajectories in case 6 start with $\varphi = \pi/2$, $\varphi = \pi$, and $\varphi = 4\pi/3$. The air parcel trajectory starting with $\varphi = \pi$ is shown in Fig. 6a where the air parcel descends from its initial position.

Model simulation results are given in Figs. 6a–d and Table 3 under case 6. As expected, the relative humidity has not reached its peak value in the very beginning. At 150 s, only a few ice crystals are nucleated. After two wave cycles (1200 s), the initial unimodal crystal spectrum (Fig. 6c) developed to a bimodal spectrum. This bimodal spectrum contains crystals from about 15 μm to 50 μm, and the spectrum is broader compared to the spectrum at 1200 s in case 1.

Air parcel trajectories starting at $\varphi = \pi/2$ and $4\pi/3$ were also simulated. For the $\varphi = \pi/2$ case, the air parcel descends almost double the distance as in the $\varphi = \pi$ case. Three nucleation events were observed in the model simulation starting at $\varphi = \pi/2$. A crystal spectrum covering a size range from 0.5 to 70 μm were produced. In the $\varphi = 4\pi/3$ case, the air parcel was exposed to a very strong uplift similar to case 2. There is no additional nucleation in this case.

From the three tests in case 6, we can see that the air parcel's starting point in a wave trajectory is a key parameter in terms of the shape and the broadness of the crystal spectra. It appears that when a wave trajectory starts at an initial position where the air parcel has a descending motion, a broader crystal spectrum could be produced without other processes, such as entrainment and aggregation, being present. Entrainment is likely to broaden crystal spectra in real clouds, but it is not the only process that can produce broad spectra.

4. Summary

In this study, a cirrus cloud microphysical parcel model (Heymsfield and Miloshevich 1989; Lin et al. 1998) has been used to study the influence of dynamics on cirrus cloud microphysics. Representative data selected from a measurement campaign carried out over southern Germany during March 1994 (Ström et al. 1997) were used for a base-case model run where the air parcel moved with a wave trajectory having a period similar to the measured Brunt–Väisälä frequency and with an amplitude of about 30 m. The amplitude of the wave (i.e., the magnitude of the vertical velocity) is the key parameter in determining the crystal number concentration. The initial starting point of the air parcel in a wave trajectory is closely related to the broadness of the crystal spectrum. However, in all six cases, the model-produced crystal spectra are narrower than typical measurement values. The major conclusions of this study are:

- In a sine wave trajectory, crystal number concentration is related to wave amplitude (i.e., the vertical velocity), especially to the amplitude of the first wave in the air parcel trajectory. Air parcel trajectories with larger amplitudes (i.e., strong vertical velocity) produce relatively higher crystal concentrations but narrower ice crystal spectra.
- After two cycles in wave trajectories, the simulated crystal spectra are narrower than typical experimental data. Additional or multiple ice crystal nucleation events could occur when the first nucleation does not produce high crystal number concentrations.
- Smoothed random walk trajectories produce similar crystal spectra to the random walk trajectories themselves. The broadness of the crystal spectra is not due to the stochastic nature of the random walk trajectory but rather the initial position of the air parcel in the wave trajectory. Entrainment is not the only way to produce broad crystal spectra.

In the future, it would be interesting to compare the influence of dynamic forcing on crystal formation including the influence of the entrainment.

Acknowledgments. We would like to thank Dr. Robert Nissen for his comments on the manuscript. Support from Dr. Richard Leaitch is appreciated.

REFERENCES

DeMott, P. J., M. P. Meyers, and W. R. Cotton, 1994: Parameterization and impact of ice initiation processes relevant to numerical model simulations of cirrus clouds. *J. Atmos. Sci.,* **51,** 77–90.

Dowling, D. R., and L. F. Radke, 1990: A summary of the physical properties of cirrus clouds. *J. Appl. Meteor.,* **29,** 970–978.

Gultepe, I., and D. O'C. Starr, 1995: Dynamical structure and turbulence in cirrus clouds: Aircraft observations during FIRE. *J. Atmos. Sci.,* **52,** 4159–4182.

Hallett, J., 1976: Measurement of size, concentration and structure of atmospheric particulates by the airborne continuous particle replicator. Rep. AFGL–TR-76–0149, 92 pp. [Available from Desert Research Institute, University of Nevada System, Reno, NV 89507.]

Heymsfield, A. J., and R. M. Sabin, 1989: Cirrus crystal nucleation by homogeneous freezing of solution droplets. *J. Atmos. Sci.,* **46,** 2252–2264.

——, and L. M. Miloshevich, 1993: Homogeneous ice nucleation and supercooled liquid water in orographic wave clouds. *J. Atmos. Sci.,* **50,** 2335–2353.

——, and ——, 1995: Relative humidity and temperature influences on cirrus formation and evolution: Observations from wave clouds and FIRE II. *J. Atmos. Sci.,* **52,** 4302–4326.

Jensen, E. J., O. B. Toon, D. L. Westphal, S. Kinne, and A. J. Heymsfield, 1994: Microphysical modeling of cirrus 1: Comparison with 1986 FIRE IFO measurements. *J. Geophys. Res.,* **99**(D5), 10 421–10 442.

Kinne, S., T. P. Ackerman, A. J. Heymsfield, F. P. J. Valero, K. Sassen, and J. D. Spinhirne, 1992: Cirrus microphysics and radiative transfer: Cloud field study on 28 October 1986. *Mon. Wea. Rev.,* **120,** 661–684.

Lin, H., K. J. Noone, J. Ström, and A. J. Heymsfield, 1998: Small ice crystals in cirrus clouds: A model study and comparison with in situ observation. *J. Atmos. Sci.,* **55,** 1928–1939.

Noone, K. B., K. J. Noone, J. Heintzenberg, J. Ström, and J. A. Ogren, 1993: In situ observations of cirrus cloud microphysical properties using the counterflow virtual impactor. *J. Atmos. Oceanic Technol.,* **10,** 294–303.

Sassen, K., and G. C. Dodd, 1989: Haze particles nucleation simulations in cirrus clouds, and applications for numerical modeling and lidar studies. *J. Atmos. Sci.,* **46,** 3005–3014.

Ström, J., and J. Heintzenberg, 1994: Water vapor, condensed water, and crystal concentration in orographically influenced cirrus clouds. *J. Atmos. Sci.,* **51,** 2368–2383.

——, ——, K. J. Noone, K. B. Noone, J. A. Ogren, F. Albers, and M. Quante 1994: Small crystal in cirriform clouds: A case study of residue size distribution, cloud water content and related cloud properties. *Atmos. Res.,* **32,** 125–141.

——, B. Strauss, F. Shröder, T. Anderson, J. Heintzenberg, and P. Wendling, 1997: In situ observations of the microphysical properties of young cirrus clouds. *J. Atmos. Sci.,* **54,** 2542–2553.

Zender, C. S., and J. T. Kiehl, 1994: Radiative sensitivities of tropical anvils to small ice crystals. *J. Geophys. Res.,* **99,** 25 869–25 880.